

Fabio V. De Blasio · Giovanni B. Crosta

# Simple physical model for the fragmentation of rock avalanches

Received: 8 September 2012 / Revised: 20 June 2013 / Published online: 29 August 2013  
© Springer-Verlag Wien 2013

**Abstract** Rock avalanches are the largest granular flows on Earth. In contrast to artificial, small-scale granular avalanches, they exhibit a large degree of fragmentation with reduction of average grain volume by a factor of up to  $10^{15}$ – $10^{18}$ . Even though fragmentation likely affects the whole dynamics of the rock avalanche, as yet the basic mechanics of the process is poorly known. In this work, a simple model is presented for the fragmentation of rock avalanches, assuming that most of the fragmentation occurs along force chains in the granular medium. The landslide motion is simulated along a curved bumpy profile path. The predicted grain spectra are found to agree reasonably with field data.

## 1 Introduction

Rock avalanches are dense granular flows ranging in volume from  $10^6$  m<sup>3</sup> to some km<sup>3</sup>. Many physical experiments have addressed the dynamics of granular materials travelling along an artificial flume (e.g., [20, 29, 30]). Aimed as small-scale models of natural rock avalanches, these experimental tests have provided valuable information about the dynamics of natural events. However, they have inherent limitations, as evident from the fact that the simulated run-out, appropriately rescaled, is still much shorter than that observed in real rock avalanches, which are capable of travelling horizontally five to even ten times their fall height (e.g., [32]). Moreover, the effective friction of rock avalanches decreases as a function of the volume [11, 15, 21, 32], in marked contrast to flume experiments, where flow resistance seems to be determined solely by the friction coefficient between the grains and the base [5, 15, 29, 30]. However, there is one even more important reason as to why flume tests are not capable of capturing key features of natural events. Rock avalanche deposits (Fig. 1a) are characterized by a dramatic degree of fragmentation which is uncommon in experiments owing to the low energy involved [4, 22]. In fact, grain size distributions in rock avalanche deposits [5] show a volume reduction of the grains by something between fifteen to eighteen orders of magnitude in volume, controlled by fall geometry, topography, environmental conditions and strength of the involved materials (see Fig. 1b). A general decrease in grain size with depth is also observed within rock avalanche deposits [4, 22] suggesting a possible dependence on normal stress and on the localization of strain in shear bands of different size and position.

A quantitative analysis and theoretical explanation of fragment size distribution of a rock avalanche deposit at different positions and depths could provide indications on the impact energies and state of stress. Moreover, the reduction in average grain size might also have an influence on the dynamics of the avalanche itself (e.g., [1, 7, 18]). As a first step toward modelling the fragmentation of a rock avalanche, we should recognize the most likely mechanism of size reduction. Although the initial collapse of a rocky mass certainly produces significant

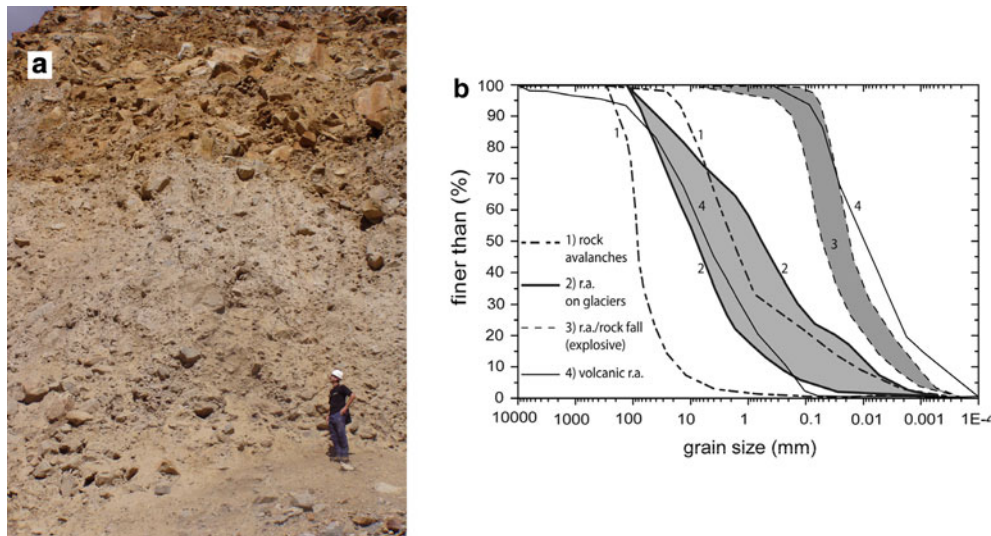


**Fig. 1** **a** The Val Pola rock avalanche deposits; **b** grain size distribution for rock avalanche deposits in different environments and materials

rapid fragmentation, as directly witnessed in the initial phases of some collapses [4, 34], natural deposits of large rock avalanches often show preservation of geological structures (e.g., relative position of materials) during the flow, signifying that not much internal displacement has taken place in the body of a rock avalanche. This is also consistent with calculations showing that inelastic dissipation in a granular avalanche causes particle–particle velocity to rapidly diminish to velocities below a few metres per second [12]. Thus, although more than one single mechanism of fragmentation is likely to occur (see e.g., a list of possible processes in [9]), a great amount of fragmentation occurs due to vertical stresses rather than to impact. Experiments and numerical modeling show that the stress in a compressed granular medium is arranged in force chains [13, 14, 26, 35]. Grains belonging to a force chain are thus subjected to a particularly intense compressive stress and are the most likely to break [25].

Despite the evident effects of disintegration of rock avalanches, the investigations of rock avalanche fragmentation have been sparse [4, 7, 22]. Measurements of the grain size spectra and their variation within the rock avalanche deposit are rarely accompanied by theoretical explanations of the observed spectra or numerical modelling of fragmentation.

In this work we propose a model for rock avalanche fragmentation based on coupled rate equations for different populations of a certain block size. The model is built on the idea that one of the principal processes of rock avalanche fragmentation occurs due to strong compressive forces through force chains in the granular medium, augmented by the effect of topographic roughness. Because our attempt is to put the problem in a quantitative perspective, the model is devised in such a way as to allow for a direct comparison with observations. Thus, synthetic spectral distributions are built and compared with field data. The intent of the work is to analyze and simulate rock fragmentation by imposing a specific rock avalanche dynamics, and geometrical slope profile both at the macro-scale (i.e. slope profile and curvature), and meso-scale (roughness or waviness). The reverse, i.e., possible influence of fragmentation on the avalanche dynamics, is not included in the model.

## 2 Modelling approach

The stress distribution in granular materials deviates markedly from the hydrostatic behavior. This is due to the fact that finite-size grains tend to form force chains within the granular medium through which the stresses reach the highest levels. In contrast, grains that by chance do not belong to a force chain experience reduced stresses lower than average, often lower than the hydrostatic limit [6, 13]. Experiments and numerical simulations [17, 23, 24] have shown that the stress distribution is a complex function that may change shape depending on the level of stress. When a granular medium is subjected to compressive stresses exceeding some

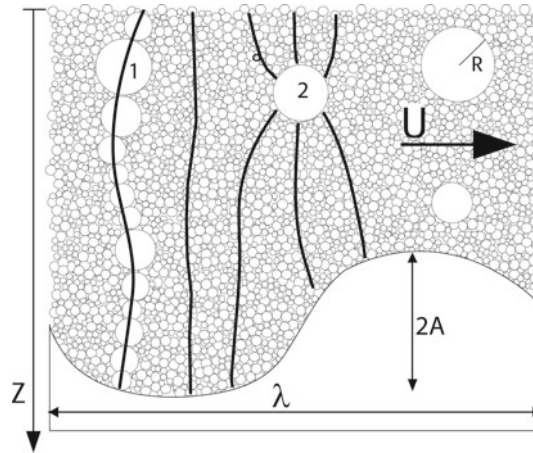


**Fig. 2** Sketch of the proposed fragmentation model. The time-dependent force distribution varies along a chain force (*case 1*). If a grain much greater than average (*case 2*) is present, the stress tends to be hydrostatic and the breakage probability diminishes. In *case 2*, more force chains intercept the block surface and the stress difference is  $\sigma_{\text{Diff}} = \sigma_{xx} - \sigma_{zz}$

MPa, the fraction of grains experiencing stresses between  $f$  and  $f + df$  follows an exponential distribution function

$$P_1(f) = \langle f \rangle^{-1} \exp[-f/\langle f \rangle], \quad (1)$$

where  $\langle f \rangle$  is the average stress at a depth  $z$  that can be assumed as the normal overburden stress tensor component averaged over all grains,  $\langle \sigma_{zz} \rangle$ . The distribution changes toward a Gaussian for higher pressures [24],

$$P_2(f) = \langle f \rangle^{-1} \exp[-(f/\langle f \rangle - 1)^2] \quad (2)$$

which is closer to the hydrostatic limit (formally, in the hydrostatic limit like that for a liquid, the stress distribution function would follow a Dirac's delta function,  $P(f) = \delta(f - \langle f \rangle)$ ). The force distribution within a moving, dense granular material has not been studied as carefully as the static case. The presence of force chains in quasi-static or slowly moving [28] and dynamic granular systems [2] has been established, to our knowledge, only in numerical models and few laboratory experiments [14]. In our model, force chains are supposed to form and dissipate continuously, as the granular medium travels onto a bumpy surface.

We assume that one spherical grain of radius  $R$  can withstand a maximum critical stress  $\sigma_f$ , beyond which it fails. Following [25] we use  $\sigma_f = \chi R^b$ , where  $\chi$  and  $b (< 0)$  are material constants. While the constant  $\chi$  is related to the hardness of the rock (the harder the rock, the more stress is needed to break it), the constant  $b$  is more involved. Physically, the negativity of  $b$  implies that a large grain has a higher probability to break. This has been related to a greater probability of a large grain to incorporate flaws within its volume, and to the fact that a higher mean stress is necessary in small particles for crack propagation [31]. The fact that fragmentation must be a dynamic process is evident from the observation that blocks at the base of static granular heaps such as talus debris and scree slopes do not break, even if often much thicker than a rock avalanche.

A portion of the landslide (Fig. 2) is assumed to travel along a terrain having the shape of an exponential slope path to which roughness is superimposed, as detailed below. For simplicity we introduce a roughness in the form of a sinusoid with fixed wavelength and amplitude so that the topographic level is

$$y(x) = \Delta H \exp(-x/\Lambda) + A \sin(2\pi x/\lambda) \quad (3)$$

where  $\Delta H$ ,  $\Lambda$ ,  $\lambda$ ,  $A$  are characteristic lengths. Whereas the quantities  $\Delta H$  and  $\Lambda$  give the maximum drop height and the characteristic slope length respectively, and thus account for the average long-range topographic features in the km-scale, the amplitude  $A$  and wave length  $\lambda$  describe the small-scale changes of the profile (i.e., roughness or waviness) in the range of tens of meters. In this way, a bump of amplitude  $A$  and wave length  $\lambda$  generates a local centrifugal acceleration of the order  $\approx \pm 4\pi^2 A U^2 / \lambda^2$ , where  $U$  is the rock avalanche velocity. Depending on the geometry and velocity, we find that the value of the acceleration may reach values greater than the Earth's gravity acceleration. The mass velocity  $U$  and position are established integrating the acceleration along slope  $a = g(\sin \beta - \mu \cos \beta)$ , where  $\mu$  is the friction coefficient giving the resistance to

sliding along the path and the local slope angle  $\beta$  is calculated from the local topography. Even if very simple, a constant friction model is often sufficient to describe the movement of the center of mass of a landslide (e.g., [11]). In Fig. 2, the number “1” shows a force chain travelling along the bumpy terrain.

Following standard formulation of comminution theory, we consider a population of spherical particles of different discrete radii,  $R_1, \dots, R_j, \dots, R_N$  where the radius  $R_j = jR_0$  is the multiple of an elementary size  $R_0$ . The generic diameter  $D_j = 2R_j$ , so that  $D_1, \dots, D_j, \dots, D_N$  are the diameters. We write our model in terms of rate theory in which the total mass  $M_i$  of rock in form of blocks of diameters between  $D_i$  and  $D_{i+1}$  evolves in time as (e.g., [19])

$$\frac{dM_i}{dt} = -k_i M_i + \sum_{j=i+1}^N b_{ij} k_j M_j, \quad (4)$$

where the  $k_i$  and  $k_j$  are the rates of transformation, and the matrix  $b_{ij}$  gives the progeny of the fragmentation process. The first term on the right hand side is the decrement in the mass of class “ $i$ ” due to fragmentation, whereas the second term gives the increase of mass in the same class due to fragmentation of all classes “ $j$ ” of greater radius,  $R_j > R_i$ .

To calculate the fragmentation rate  $k_i$ , let us assume for the moment that fragmentation occurs only along the force chains. It is reasonable to expect that it will be proportional to the fraction of compressive stresses that are greater than the breaking limit  $\sigma_f$ . Because  $\int_{\sigma_f}^{\infty} P(f)df$  is the normalized number of compressive stresses greater than  $\sigma_f$ , where  $P(f)$  is the stress distribution in the granular medium seen earlier, while  $\int_0^{\infty} P(f)df$  is the number of all compressive stresses (greater or lower than  $\sigma_f$ ), it is reasonable to calculate the fragmentation rate as proportional to their ratio, namely

$$k_i^0 = \frac{1}{\tau} \frac{\int_{\sigma_f}^{\infty} P(f)df}{\int_0^{\infty} P(f)df}, \quad (5)$$

where  $\tau$  is a characteristic time over which fragmentation can occur and the superscript “0” indicates that this rate accounts only for fragmentation that occurs in force chains. This approximation may be good for grains of the same size, but becomes worse if one grain has radius much greater than that of the surrounding grains. Thus, we will introduce the possibility to differentiate this case (starting from the discussion in correspondence of Eq. (8)). Notice that the dependence on the block diameter is contained in the stress  $\sigma_f$ , since as seen earlier,  $\sigma_f = \chi R^b$  [25]. In the pressure regime investigated in the present work, pressures involved are much greater than some MPa. For this reason we choose  $P(f) = P_2(f)$ , and after some manipulation it is found that (Appendix 1)

$$k_i^0 = \frac{1}{\tau} \frac{1 - \operatorname{erf}\left(\frac{\sigma_f}{\sigma_{zz}} - 1\right)}{1 + \operatorname{erf}(1)}, \quad (6)$$

where  $\operatorname{erf}(\dots)$  denotes the error function. The time  $\tau$  of disintegration is taken to be the longest of the characteristic times involved in the processes of breakage and re-ordering of the force chains. Because the breakage time is short ( $\ll 1$  ms),  $\tau$  is close to the time needed for grains to travel a vertical distance of the order of the grain size. A simple estimate for the vertical speed of the grains gives  $U = VT/L$ , where  $V$  is the horizontal speed of the landslide,  $T/L$  is the ratio between landslide thickness and length, ca. 1/100. With a relative velocity of the order 10–50  $\text{ms}^{-1}$ , it is reasonable to assume  $\tau$  of the order 10–30 ms. The progeny matrix  $b_{ij}$  has been calculated based on the mixed logarithmic distributions practical for crusher machines as explained by [19]  $b_{ij} = B(R_i - 1; R_j) - B(R_i; R_j)$ , where (Appendix 2)

$$B(R_i; R_j) = K \left(\frac{R_i}{R_j}\right)^{N_1} + (1 - K) \left(\frac{R_i}{R_j}\right)^{N_2} \quad (7)$$

is an empirical breakage function providing the cumulative distribution in terms of two populations, that fits well empirical data [19]. In Eq. (7),  $N_1 = 0.45$ ,  $N_2 = 3.2$ ,  $K = 0.3$  are materials constants [19]. Conservation of the total mass is ensured requiring  $B(R_1; R_j) = 0$  for all  $j$ , where  $R_1$  is the smallest radius of the particle distribution.

So far we have considered all grains of the same size in the force chains. However, as fragmentation proceeds, grains acquire different sizes. In principle, we could expect that a significant deviation from the stress

formulas (Eqs. 1 and 2) occurs when a block is much greater than the average ambient block. Let us consider a block of radius  $R$  immersed in a medium of blocks with radius  $r \ll R$ . In this limit, the large block experiences an average stress close to the hydrostatic limit (or quasi-hydrostatic as it is not isotropic)  $\sigma_{xx} \neq \sigma_{zz}$  and the block is crushed by the stress difference between vertical and horizontal stress  $\sigma_{\text{Diff}} = \sigma_{xx} - \sigma_{zz}$ . The  $xx$  component of the stress tensor is related to the  $zz$  component by the earth pressure coefficient  $K_{\text{EP}}$ :  $\sigma_{xx} = K_{\text{EP}}\sigma_{zz}$  [27]. If we choose  $K_{\text{EP}}$  corresponding to rupture limit, and introducing the internal friction angle  $\varphi$  of the material, we find  $\sigma_{\text{Diff}} = \pm 2 \sin \varphi \sigma_{zz} / (1 \pm \sin \varphi)$  where the  $\pm$  sign refers to the active ( $\sigma_{xx} < \sigma_{zz}$ ) and passive ( $\sigma_{xx} > \sigma_{zz}$ ) states, respectively. In a moving rock avalanche the state probably changes frequently from active to passive following the topographic features. Considering that most rock avalanches stretch during the flow, probably the active state is prevalent. However, for landslides moving on complex topographies, like the Val Pola rock avalanche [4], the collapse onto a flat region and the presence of the opposite side of the valley could generate a passive state. The same thing could happen where sudden changes in topographic gradient or the presence of softer materials induce a decrease in velocity or a stoppage of the front.

In the calculations, we implement on the possibility that a block be much larger than the ambient blocks and so write the rate of fragmentation as

$$k_i = k_i^0 \gamma_i + (1 - \gamma_i) \frac{\Gamma}{\tau} \Theta(\sigma_{\text{Diff}} - \sigma_f), \quad (8)$$

where  $\Gamma \approx 1$  is a coefficient to rescale the characteristic time for large isolated blocks,  $K_i = (\Gamma/\tau) \Theta(\sigma_{\text{Diff}} - \sigma_f)$  is the rate of fragmentation due to the nearly hydrostatic behaviour where  $\Theta(\dots)$  is the Heaviside function and  $\gamma_i = \exp\{-\alpha [(R_i - \langle R \rangle) / \langle R \rangle]^2\}$ , where  $\alpha$  is a constant and  $\langle R \rangle$  is the average grain radius. For a block of radius  $R_i$  much larger than the average radius  $\langle R \rangle$ , the factor  $\gamma_i$  (expressing the probability of failure of blocks of size  $R_i$ ) becomes small which reduces the probability for the block to fail. In the opposite situation  $R_i \approx \langle R \rangle$ , the rate  $\gamma_i \approx 1$  and fragmentation occurs along force chains.

### 3 Results and discussion

The calculation is started with initial abundances  $M_i = 0$  except for the ten largest size classes  $M_{N-9}, M_{N-8}, \dots, M_N$  of unitary mass. A total  $10^4$  classes of radius, each one with a fixed grain size (radius) increment of 0.03 mm, was considered. Abundances are then calculated in time with Eq. (4) using the Eqs. (4–8) at discrete time steps. Figure 3 sketches the rate model used in this work. A counter “ $i$ ” records a certain mass  $M_i$  of grains of radius  $R_i$ ; at each time step the amounts  $M_i$  of each counter are updated with the coupled rate equations.

For the calculations we have chosen different slope geometries. We show results for a “gentle” profile ( $\Lambda = 1250$  m), and a “steep” profile ( $\Lambda = 1110$  m), reproduced in the top panel of Fig. 4 together with the velocity as a function of the position and time ( $\Lambda$  controls the rate of decrease in altitude). Although the profiles are not tremendously different, the square of the velocity (which is the term appearing in the fragmentation equation) changes much more rapidly to produce different behaviour in the two cases. Indeed, these two profiles emphasize the transition between moderate to strong fragmentation. A further problem that needs to be accounted for in the simulation, is the decrease in thickness of the landslide (the landslide “stretching”), which has an important consequence on the internal pressures. In a complete model, stretching itself should follow from the dynamics. Because the present work deals with the production of fragments and not with the

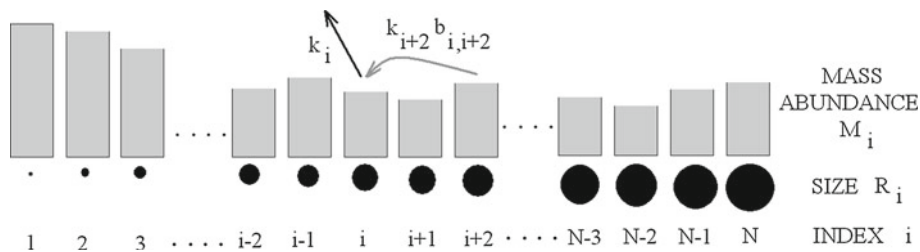


**Fig. 3** Sketch of the computational model. There are  $N$  size classes and at each time step the mass abundance of a certain class “ $i$ ” (represented with grey rectangles) is updated in Eq. (4) based on the inflow from the breakage of grains from greater size classes  $i + 1, i + 2, \dots, N$  (grey arrow) and outflow to smaller classes  $i - 1, i - 2, \dots, 1$  (black arrow)



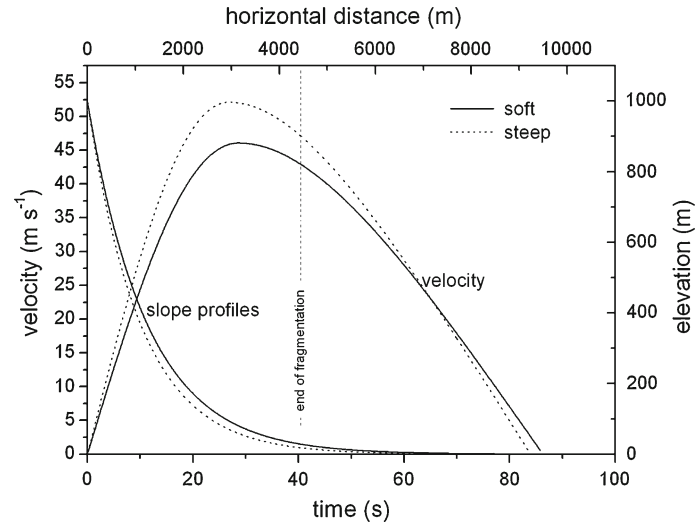


**Fig. 4** Velocity ( $U$ ) calculated for two different slope profiles. The avalanche is assumed to translate rigidly along an exponential slope path of the form  $y(x) = \Delta H \exp(-x/\Lambda)$  ( $\Delta H = 1$  km,  $\Lambda = 1.25$  km;  $\mu = \tan \phi = \tan(22^\circ) = 0.404$  and  $\Delta H = 1$  km,  $\Lambda = 1.11$  km;  $\mu = 0.404$ )

feedback effect that fragmentation has on the further dynamics (which is, moreover, poorly known) we impose the stretching externally, stipulating that the thickness  $T$  decreases as a function of the path  $L$  as  $T = T_o(L_o/L)$ . As a partial justification, note that in some cases the dynamics of rock avalanches can be successfully described as the motion of the center of mass of a frictional material whose body is stretching proportionally to the travel distance during the motion [12, p. 196]. In our example,  $T_o = 150$  m and  $L_o = 400$  m are the initial thickness and length.

Fragmentation requires that the moving mass travels at velocities greater than a critical speed, which is a function of the state of stress (i.e. depth). The grain size curves obtained at growing times are shown in Fig. 5. The data presented show the case for the two different slope profiles, and for two different values of the parameter  $\alpha$  (in Eq. (8), 0.3 and 0.03). In the case of  $\alpha = 0.3$ , fragmentation occurs both along the force chains and due to hydrostatic load, while at small  $\alpha = 0.03$  fragmentation occurs along the force chains rather than due to hydrostatic load. Each simulation is superimposed to the Val Pola data for samples at depths of 15 and 50 m but can be easily compared with data in Fig. 1b from various rock avalanche deposits. We have chosen this rock avalanche deposit because it is one for which a detailed grain size spectrum is available [3,4], for points located both at different depths within the deposit and distances from the source areas. The Val Pola rock avalanche occurred on 28 July 1987 in the upper Valtellina (Lombardy, Northern Italy), and developed crossing and occupying a large sector of the valley bottom causing 27 casualties, and destroying three villages. The rock avalanche was originated from an old rockslide body which was clearly delimited by an upper steep scarp area, and developing within highly fractured and tectonized metamorphic rocks. The original mass, estimated between 34 and 43 millions of cubic meters, sled down the valley flank (mean slope of  $34^\circ$ ) scraping 5 to 8 millions of cubic meters of debris along the path, reached the valley bottom and ran 300 m up the opposite valley flank, for a maximum drop height of about 1,200 m. The rock avalanche mass slip into two main lobes of length 1 and 1.5 km flowing respectively upstream and downstream along the valley bottom. The final deposit reached a maximum thickness of 90 m and the farthest deposit tip came to rest at a distance of about 3.6 km from the upper scarp area. The total duration of the event (70–120 s) was recorded by a series of seismograph stations in Italy and Switzerland at distances between 37 and 248 km. The deposit of poorly sorted material was characterized by ridges and furrows parallel to the valley axis, lobate forms, large blocks prevalently at the deposit surface and fine grained materials within the main accumulation body. Large blocks were abundant at the surface reaching some tens of meters in size; the abundance of boulders and gravel by volume was found to be between 8 and 95 %, sand ranged between 10 and 75 %, whereas silt and clay was between 6 and 60 %.

Figure 5a reports the results for a gentle profile. At the beginning of the simulation (10 s) the grain size distribution has changed little from the initial configuration; after 20 s, however, the spectrum changes to smaller grains, but without much difference between the case of  $\alpha = 0.3$  (red) and 0.03 (blue). The curve at

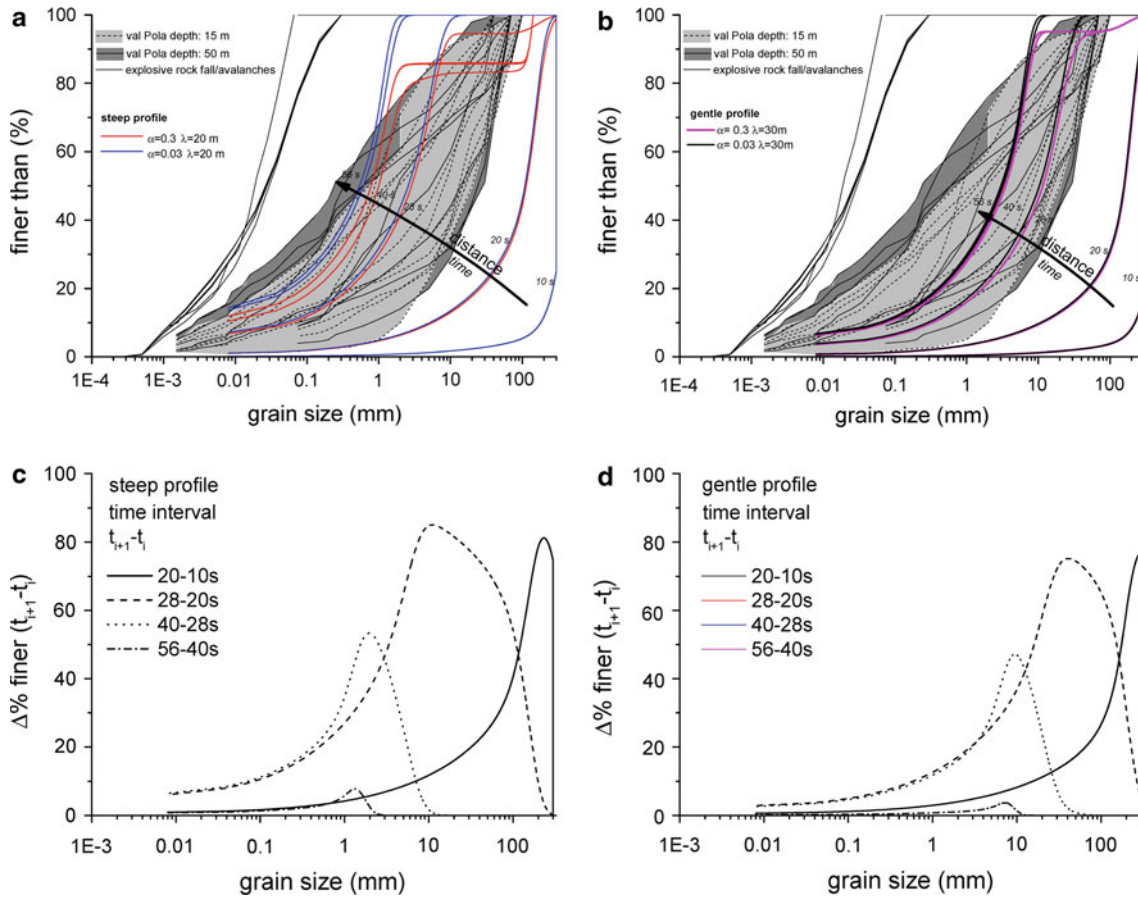


**Fig. 5** Integral grain spectra computed at different times for the steep and the gentle slope profiles (see Fig. 3, computation input data: time step = 0.04 s;  $A = 0.5$  m,  $\alpha = 0.05$ ;  $\log_{10} \chi$  (Pa) = 6.4;  $b = -0.343$ ;  $N_1 = 0.45$ ;  $N_2 = 3.2$ , [19]). Simulation results for  $\lambda = 20$  m with gentle profile, and  $\lambda = 30$  m with steep profile are compared to grain size distributions from real rock avalanches. Distributions are reported at the following times from start of failure: 10, 20, 28, 40, 56 s (after which fragmentation ends). Superimposed to the model results, we report the integral distribution spectra for the Val Pola rock avalanche measured in the final deposit at depths of 15 and 50 m, together with the measurements for explosive rock avalanches. Notice that fragmentation extends to smaller grain sizes at 50 m rather than at 15 m depth in the body of the Val Pola. Note also the large dispersion of the data

28 s shows a start toward much fragmentation. The curve with  $\alpha = 0.03$  increases uniformly to unity as a function of the grain size, while that with  $\alpha = 0.3$  starts developing a plateau for large grains. After 56 s, all possible fragmentation has taken place in the model, and the spectrum does not change anymore.

Looking at panel b of Fig. 5 for the results on a steep profile, we note how in this case, the sliding creates a more pronounced fragmentation, where grains with size greater than 2 mm are absent from the final state. In both simulations, the distributions obtained with a high value of  $\alpha$  result in a plateau for large blocks, in apparent contradiction with field data. This is understandable considering that a large value for  $\alpha$  implies that large blocks which have survived an early fragmentation stage, cannot be accommodated along a force chain, and may break only hydrostatically. Panels c and d show the difference in spectral distributions between successive times. The figure emphasizes a progressive shift of fragmentation toward small grain size and a final flattening of the curves, when fragmentation is ended.

Directly comparing the simulations with data, the “best” prediction would be the one with a small value ( $\alpha = 0.03$ ) and gentle profile. In this case, the results show a satisfactory agreement with the observed curves, as both the typical grain size interval and the progressive increase in fines is well simulated. This could imply that very few blocks are broken hydrostatically, and most fragmentation occurs along force chains. However, given the approximations involved and the high uncertainties, it is more reasonable at the present stage to focus on the general trends rather than the specific prediction. Note that fragmentation proceeds steadily but reaches a limit after which it stops. Thus, fragmentation on a steep slope will proceed faster at the beginning of sliding

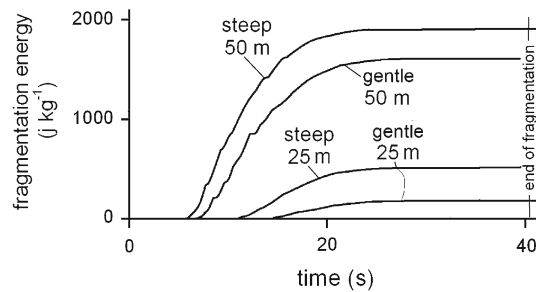


**Fig. 6** Computed fragmentation energy for different slope profiles (see Fig. 3) and constant depth as a function of time. Input data as in Fig. 4. Note that “gentle” profile under a constant load of 15 m does not produce fragmentation

and stop early, whereas on gentler slopes the fragmentation process will be more gradual. Such a decrease in total fragmentation with distance has been observed for the Val Pola rock avalanche [4]. Figure 4 also reports the grain spectrum resulting from explosive impact, occurring when rock falls hit the topographic surface at high speed ( $100\text{--}150\text{ m s}^{-1}$ ) with production of a dust cloud. The resulting size spectrum is much finer and more uniform than for rock avalanches, probably reflecting the size of the rock crystals.

Figure 6 shows the fragmentation energy as a function of time calculated with Bond’s model for fragmentation energy [19,31] under an initial thickness (25 and 50 m) for the gentle and steep profiles. Bond’s is a model devised in comminution engineering to control and reduce the power needed by crushers, mills, and high-velocity impact equipments. According to the Bond’s model, if the fragmentation of a granular medium with size spectrum such that 80% of the grains are larger than a diameter  $D$  leads to a new spectrum where 80% of the grains are smaller than  $d \ll D$ , the corresponding fragmentation energy is  $E = 0.01W(1/\sqrt{d} - 1/\sqrt{D})$  where  $D$  and  $d$  should be expressed in cm. The parameter  $W$ , known as the work Bond index, is a characteristic of the rock to be determined empirically; it represents the energy per mass necessary to fragment the rocky material from infinite size ( $D \rightarrow \infty$ ) to the 80% sieve size of 100 microns ( $d = 10^{-4}$  cm). In some refined calculations, this index is itself considered a smooth function of the particle size, even though we have kept it constant in the calculations. The larger this index, the more energy is needed for fragmentation. For example, the values for a soft rock like gypsum, for intermediate-hardness rock like limestone, and a hard rock like gneiss are about 38, 47, and 81  $\text{kJ kg}^{-1}$ , respectively [31,33]. The Bond’s model, with its dependence on the square root of the particle size, has no straightforward physical interpretation, yet it appears reasonably accurate for intermediate-size particles, and is widely used [19]. It should be stressed that even under the strict experimental control, fragmentation energy may depend on the way fragmentation occurs (e.g., crushing versus high-velocity impact) and even on the design of the comminution machine [19,33] and so the boundary conditions. The energy calculated with our model is found to be 4–7% of the gravitational energy, which indicates that fragmentation appears to be a minor energy sink for rock avalanches [4,12,22].

## 4 Conclusions

We have proposed a simple model for the fragmentation of a rapid rock avalanche. In its simplicity, the model introduces the effects of the fragmentation along force chains moving on rough terrain, linking them to slope geometry characteristics and the speed of the centre of mass. For a wavy surface the local slope curvature can control the degree of fragmentation and thus the final grain size distribution within the deposit. Naturally-forming force chains in a granular medium are capable of focalizing stress concentration, and are more significant than particle–particle impacts in bulk fragmentation of a landslide.

Fragmentation is perhaps the most evident characteristic of a rock avalanche deposit, and the lack of a model to understand how it occurs certainly hampers our understanding of the dynamics of these natural hazards. Many large rock avalanches such as Koefels and Flims respectively in Austria and Switzerland, show “in place” geological structures in the landslide deposit [16]. This suggests that despite the complete fragmentation of rock (the deposit appears powdery), there has not been relative displacement of the parts, which indicates a vertically-driven fragmentation process like the one examined here, rather than shear and impact fragmentation, at least for some parts of these thick rock avalanches. In addition of being a “stress indicator”, fragmentation might play a role in the dynamics of the landslide itself. Fragmentation could promote landslide mobility [7,8] but in some ways that still needs to be fully understood, considering that it is an energy-consuming process.



One possibility indicated by small-scale experiments is that mobility could be enhanced by the presence of sudden topographic changes coupled with fragmentation [1]. Alternately, fragmentation in the presence of water could result in a lubricating fluid of non-Newtonian properties [10], but this needs to be experimentally demonstrated.

The most important suggestion of the present work is perhaps the characterization of rock avalanche fragmentation built with coupled rate equations like in Eq. (4). As yet, however, much remains to be done to describe the relevant kinetic and parameters to be used in the coupled equations. A more complete model of landslide fragmentation based on the kinetics of the processes should also include the process of shearing fragmentation and superficial chipping that forms the dust commonly observed in rock avalanches.

### Appendix 1: details on the calculation of Eq. (2)

Remembering the definition of the error function  $\text{erf}(x) = \frac{2}{\sqrt{\pi}} \int_0^x \exp(-y^2) dy$ , THE integrals in the ratio  $k_i = \left[ \int_{\sigma_f}^{\infty} P(f) df \right] \left[ \int_0^{\infty} P(f) df \right]^{-1}$  with  $P(f) = P_2(f)$  become  $\int_{\sigma_f}^{\infty} P_2(f) df = \langle f \rangle^{-1} \int_{\sigma_f}^{\infty} \exp \left[ -(f/\langle f \rangle - 1)^2 \right] df = (\sqrt{\pi}/2) [1 - \text{erf}(\sigma_f/\sigma_{zz} - 1)]$  and  $\int_0^{\infty} P_2(f) df = (\sqrt{\pi}/2) [1 - \text{erf}(-1)] = (\sqrt{\pi}/2) [1 + \text{erf}(1)]$  where, as explained in the text, we made the identification  $\langle f \rangle = \sigma_{zz}$  for the diagonal part of the macroscopic stress (the overburden pressure). Further division by the characteristic time  $\tau$  provides Eq. (6).

### Appendix 2: breakage function

Because in our model we employed concepts from the rather specialized field of comminution industry where rock fragmentation is being studied quantitatively, it can be useful to summarize here some of these notions. The need to describe the size classes during the process of comminution has led to a series of models that can fit the data fairly well, even though such models are often totally empirical [19]. In any model of rock avalanche fragmentation that aims at comparing the theoretical prediction with data, it becomes of great importance to model the size of the progeny (“daughter particles”) following the breakage of one single block. A popular model describes the progeny in terms of a mixture of two populations of small and large size. One thus defines a cumulative distribution function of progeny  $B(R_i; R_j)$  as the fraction of daughter particles smaller than  $R_i$  resulting from the breaking of a particle of size  $R_j$ . Empirically, each of the two populations follows a distribution of the form  $B(R_i; R_j) \propto (R_i/R_j)^N$ , where  $N$  is a constant. For  $N \ll 1$ , the distribution is skewed towards very small particles (fragmentation leads to powder), while a greater value leads to larger daughter particles. The empirical observation of two prevalent sizes in the progeny is modeled as the sum of two distributions like in Eq. (3) with a different exponent  $N$  and with a weighing parameter  $K$  for the total progeny distribution. These are the cumulative distributions as measured in the comminution machines. The differential parameter needed to calculate the progeny to a single size class must be calculated as the difference,  $b_{ij} = B(R_i - 1; R_j) - B(R_i; R_j)$ .

### References

1. Bowman, E.T., Take, W.A., Rait, K.L., Hann, C.: Physical models of rock avalanche spreading behaviour with dynamic fragmentation. *Can. Geotech. J.* **49**, 460–476 (2012)
2. Cleary, P.: Modelling comminution devices using DEM. *Int. J. Numer. Anal. Methods Geomech.* **25**(1), 83–105 (2001)
3. Crosta, G.B., Chen, H., Lee, C.F.: Replay of the 1987 Val Pola Landslide, Italian Alps. *Geomorphology* **60**(1–2), 127–146 (2004)
4. Crosta, G.B., Frattini, P., Fusi, N.: Fragmentation in the Val Pola rock avalanche, Italian Alps. *J. Geophys. Res.* **112**, F01006 (2007). doi:[10.1029/2005JF000455](https://doi.org/10.1029/2005JF000455)
5. Crosta, G.B., Imposimato, S., Roddeman, D.: Numerical modeling of 2-D granular step collapse on erodible and non erodible surface. *J. Geophys. Res.* **114**, F03020 (2009). doi:[10.1029/2008JF001186](https://doi.org/10.1029/2008JF001186)
6. Dantu, P.: Etudes statistique des forces intergranulaires dans un milieu pulvérulent. *Geotechnique* **18**, 50–55 (1968)
7. Davies, T.R.H., McSaveney, M.J.: The role of dynamic rock fragmentation in reducing frictional resistance to large landslides. *Eng. Geol.* **109**, 67–79 (2009)
8. Davies, T.R., McSaveney, M.J., Deganutti, A.M.: Dynamic fragmentation causes low rock-on-rock friction. In: Proceedings of 1st Canada–U.S. Rock Mechanics Symposium, Vancouver, Canada, pp. 27–31 (2007)

9. De Blasio, F.V.: A simple dynamical model of landslide fragmentation during flow. In: Senneset, K., Flaate, K., Larsen, J.O. (eds.). *Landslides and Avalanches: ICFL 2005 Norway*. Taylor and Francis, London, pp. 95–100 (2005)
10. De Blasio, F.V.: Rheology of a wet, fragmenting granular flow and the riddle of the anomalous friction of large rock avalanches. *Granul. Matter* **11**, 179–184 (2009). doi:[10.1007/s10035-009-0134-6](https://doi.org/10.1007/s10035-009-0134-6)
11. De Blasio, F.V.: *Introduction to the Physics of Landslides*. pp. 408 Springer, Berlin (2011)
12. De Blasio, F.V.: Dynamical stress in force chains of granular media travelling on a bumpy terrain and the fragmentation of rock avalanches. *Acta Mechanica* **221**, 375–382 (2011)
13. Duran, J.: *Powders and Grains*. Springer, Berlin, p. 214 (2003)
14. Estep, J., Dufek, J.: Substrate effects from force chain dynamics in dense granular flows. *J. Geophys. Res.* **117**, F01028 (2012). doi:[10.1029/2011JF002125](https://doi.org/10.1029/2011JF002125)
15. Erismann, T.H., Abele, G.: *Dynamics of Rockslides and Rockfalls*. pp. 316 Springer, Berlin (2001)
16. Erismann, T.H.: Flowing, bouncing, sliding: synopsis of basic mechanisms. *Acta Mechanica* **64**, 101–110 (1986)
17. Howell, D., Behringer, R.P., Veje, C.: Stress fluctuations in a 2D granular Couette experiment: a continuous transition. *Phys. Rev. Lett.* **82**(26), 5241–5244 (1999)
18. Imre, B.: *Micromechanical analyses of sturzstroms (rock avalanches) on Earth and Mars*. Report no. 241, Swiss Federal Institute of Technology, Zurich (2012)
19. King, R.P.: *Modeling and Simulation of Mineral Processing Systems*. pp. 403 Butterworth Heinemann, Boston (2001)
20. Lajeunesse, E., Mangeney-Castelnau, A., Viotte, J.P.: Spreading of a granular mass on a horizontal plane. *Phys. Fluids* **16**, 2371–2382 (2004)
21. Legros, F.: The mobility of long-runout landslides. *Eng. Geol.* **63**(3–4), 301–331 (2002)
22. Locat, P., Couture, R., Locat, J., Leroueil, S., Jaboyedoff, M.: Fragmentation energy in rock avalanches. *Can. J. Geotech.* **43**, 830–851 (2006)
23. Lube, G., Huppert, H.E., Stephen, R., Sparks, J., Freundt, A.: Collapses of two-dimensional granular columns. *Phys. Rev. Lett.* **72**(041301), 1–10 (2005)
24. Makse, H.A., Johnson, D.L., Schwartz, L.M.: Packing of compressible granular materials. *Phys. Rev. Lett.* **84**, 4160–4163 (2000)
25. McDowell, G.R., Bolton, M.D.: On the micro-mechanics of crushable aggregates. *Geotechnique* **48**, 667–679 (1998)
26. Mueth, M., Jaeger, H.M., Nagel, S.R.: Force distribution in a granular medium. *Phys. Rev. E* **57**, 3164–3169 (1998)
27. Nedderman, R.M.: *Statics and Kinematics of Granular Materials*. pp. 352 Cambridge University Press, Cambridge (1992)
28. Pena, A.A., Herrmann, H.J., Lind, P.G.: Force chains in sheared granular media of irregular particles. *AIP Conf. Proc.* **1145**, 321–324 (2009)
29. Pouliquen, O., Forterre, Y.: Friction law for dense granular flows: application to the motion of a mass down a rough inclined plane. *J. Fluid Mech.* **453**, 133–151 (2002)
30. Pudasaini, S.P., Hutter, K.: *Dynamics of Rapid Flows of Dense Granular Avalanches*. pp. 626 Springer, New York (2007)
31. Rhodes, M.: *Introduction to Particle Technology*. Wiley, Chichester (1998)
32. Scheidegger, A.E.: On the prediction of the reach and velocity of catastrophic landslides. *Rock Mech.* **5**, 231–236 (1973)
33. Snow, R.H., Allen, T., Ennis, B.J., Litster, J.D.: Size reduction and size enlargement. In: Green, D. Perry's *Chemical Engineers Handbook*, Section 20, pp. 98 McGraw-Hill, New York (1997)
34. Sosio, R., Crosta, G.B., Hungr, O.: Complete dynamic modeling calibration for the Thurwieser rock avalanche (Italian Central Alps). *Eng. Geol.* **100**(1–2), 11–26 (2008)
35. Tordesillas, A., Walker, D.M., Lin, Q.: Force cycles and force chains. *Phys. Rev. E* **81**, 011302 (2010)